Magnetic Surfaces and Localized Perturbations in the Wendelstein VII-A Stellarator

H. Wobig

IPP 2/283 September 1986

MAX-PLANCK-INSTITUT FÜR PLASMAPHYSIK

8046 GARCHING BEI MÜNCHEN

MAX-PLANCK-INSTITUT FÜR PLASMAPHYSIK

GARCHING BEI MÜNCHEN

Magnetic Surfaces and Localized Perturbations in the Wendelstein VII-A Stellarator

H. Wobig

IPP 2/283 September 1986

Die nachstehende Arbeit wurde im Rahmen des Vertrages zwischen dem Max-Planck-Institut für Plasmaphysik und der Europäischen Atomgemeinschaft über die Zusammenarbeit auf dem Gebiete der Plasmaphysik durchgeführt.

MAGNETIC SURFACES AND LOCALIZED PERTURBATIONS IN THE WENDELSTEIN VII-A STELLARATOR

H. Wobig

Max–Planck–Institut für Plasmaphysik, EURATOM Association
D-8046 Garching, FRG

Abstract

The critical dependence of plasma confinement in low-shear stellarators, such as Wendelstein VII-A, on the external rotational transform can be explained on the basis of magnetic surface destruction. External symmetry-breaking perturbations generate islands on the low order rational magnetic surfaces. The islands are largest at $\iota = 1/2$ and $\iota = 1/3$. Confinement is optimum in close proximity to these values. In order to study the structure of surfaces under the influence of perturbations, a mapping procedure is used instead of field line integration. It is found that the neighbourhood of low- order rational surfaces is particularly robust against surface destruction. The reason is that in this vicinity only rational surfaces with large m and n exist ($\iota = m/n$). On these surfaces the external perturbation only generates small islands.

In W VII-A the current leads to the helical windings are one symmetry- breaking perturbation, and there might also be others. It is possible to avoid field errors of this kind in future stellarators.

I. Introduction

Experiments in low-shear stellarators like W VII-A /1/ exhibit a critical dependence of the plasma confinement on the structure of the magnetic field. At particular values of the rotational transform ι ($\iota = 1/2, 1/3, 2/5, ...$) confinement is deteriorated, which indicates that around these low-order rational values of ι magnetic surfaces are destroyed by perturbation fields. The experimental results indicate that the perturbation breaks the five fold symmetry of the configuration and therefore can be explained by field errors coming from the coil system. Numerical calculations /2/ have indeed shown that current leads to the helix create a local perturbation field of $10-20$ G, which gives rise to island formation on rational surfaces. The largest islands occur at $\iota = 1/2$, three smaller islands at $\iota = 1/3$ and five islands at $\iota = 2/5$. Islands are also found at $\iota = 3/7$ and $\iota = 3/8$. It is not surprising to find enhanced plasma losses in the presence of such islands. As can be seen from fig. 1 and 2 the energy content of the plasma is a minimum at $\iota = 1/2, 1/3, 2/5, 2/3, ...$.

What is surprising, however, is the maximum energy content in close proximity to $\iota = 1/2$ and $\iota = 1/3$. There is a small positive shear in WVII-A so that under these conditions the rotational transform ranges from $\iota = 0.48$ on the magnetic axis to $\iota = 0.49$ on the plasma boundary. A similar situation is $\iota = 0.51$ on the axis and 0.52 on the boundary. As already shown by numerical calculations the surfaces close to $\iota = 1/2$ or $\iota = 1/3$ are not destroyed by the perturbation which creates large islands at $\iota = 1/2$ or $1/3$. This can be understood from the distribution of rational numbers in the vicinity of $\iota = 1/2$ or $1/3$. Close to $1/2$ only rational numbers m/n exist with relatively high values of m and n. The distribution of rational numbers is shown in fig. 3, where $|log\, 1/n|$ is plotted vs $\iota = m/n$[1]. An ι -interval from $\iota = 0.48$ to 0.49 contains rational surfaces with larger values of m and n than the region from $\iota = 0.44$ to $\iota = 0.45$. A magnetic field perturbation $\mathbf{B_1}$, which is created internally or externally, contains several Fourier harmonics, which are in resonance at $\iota = m/n$ and create a chain of at least n islands. With a decreasing perturbation spectrum, we expect the size of islands to decrease strongly with the period n (n is the number of toroidal transits before the magnetic island closes upon itself). This general behaviour may explain why the neighbourhood of low-order rational surfaces is especially robust against destruction.

The perturbations from the helix leads and joints are the only ones to be identified in the WVII-A device. Other unknown error fields could also be present in the coil arrangement or originate from ferromagnetic or paramagnetic material. The particular role of $\iota = 1/2$ and $\iota = 1/3$ can only be explained by a symmetry-breaking external perturbation, otherwise $\iota = 5/n$ should be the surfaces to be destroyed first. The basic periodicity of the WVII-A stellarator is $m = 5$.

The main question now is whether the neighbourhood of low-order rational surfaces is always the last one to be destroyed by any external or internal perturbation. In order to study the structure of perturbed magnetic surfaces, field line tracing would be the appropriate method, however, but great numerical effort is required. The mapping technique developed by J. Greene /3//4/ and B. Chirikov/5/ needs much less compu-

[1]This figure has been prepared by I. and W. Ott

ter time. The disadvantage is that in general the analytic representation of the map corresponding to a perturbation field $\mathbf{B_1(x)}$ is not known, approximations have to be found. But it is well-known that any toriodal magnetic field with field lines returning to the poloidal plane after a toroidal transit provides a flux-conserving map of the poloidal plane onto itself. Studying the features of a flux (or area) conserving two-dimensional map is therefore equivalent to investigating toroidal flux surfaces with small perturbations. The theory of flux-conserving maps is well established. The KAM theorem states that irrational magnetic surfaces remain unperturbed if the perturbation is small enough /9/. Most theories of flux-conserving maps concentrate on the transition to chaos and the intrinsic scaling laws. In this context the question will be treated how configurations with different ι -regime react on a fixed perturbation.

II. Basic Equations

We start from a magnetic field $\mathbf{B_o}$ and assume the existence of nested toroidal magnetic surfaces $\psi = const.$ The field may be a vacuum field or a finite-β equilibrium field. Let the unperturbed magnetic field $\mathbf{B_o}$ be represented in flux coordinates (ψ, θ, ϕ) with the toroidal and poloidal coordinates ϕ and θ:

$$\mathbf{B_o} = \nabla\psi \times \nabla(\iota\phi - \theta) \tag{1}$$

The rotational transform $\iota(\psi) = \iota_o + \iota_1\,\psi + \iota_2\psi^2$ is specified by three constants $\iota_o, \iota_1, \iota_2$. In the poloidal plane with (ψ, θ) coordinates the twist map $T_o : \psi_1 = \psi_o\,;\ \theta_1 = \theta_o + 2\pi\,\iota(\psi_1)$ yields the Poincaré plot of the unperturbed surfaces. The unperturbed surfaces are circles in this coordinate system. The perturbation field $\mathbf{B_1}$ leads to a perturbed map $T_o + T_1$ which can be derived from a generating function

$$S(\psi_1, \theta_o) = \psi_1\,\theta_o + 2\pi \int^{\psi_1} \iota(\psi) d\,\psi + h(\psi_1, \theta_o) \tag{2}$$

by

$$\psi_o = \frac{\partial S}{\partial \theta_o} \quad ; \quad \theta_1 = \frac{\partial S}{\partial \psi_1} \tag{3}$$

Owing to this procedure the determinant of the transformation is unity and the magnetic flux is automatically conserved. The function $h(\psi_1, \theta_o)$ represents the effect of the perturbation field $\mathbf{B_1}$. In general the relation between $\mathbf{B_1}$ and $h(\psi_1, \theta_o)$ is unknown, except in the case of a perturbation localized in the toroidal angle ϕ. With such δ-like dependence the field line equations can be integrated explicitly to yield the action-generating function $h(\psi_1, \theta_o)$.

In order to study the effect of perturbations in the W VII-A stellarator ,the following ansatz for $h(\psi_1, \theta_o)$ is made: $h = \psi_1\, g(\theta_o)$ where g is a Fourier series in $sin\, l\theta_o$ $(l = 1, 2...15)$. This map roughly corresponds to an external error field which decreases towards the magnetic axis. The Fourier coefficients of $g(\theta_o)$: $K_1, ..., K_{15}$ are the control parameters of the map. With this model the following questions can be studied :

How are magnetic surfaces destroyed by increasing the control parameters?
What regime in ϵ is most resistant to destruction?

III. Localised Perturbations

In general the relation between the perturbed map $T_o + T_1$ can only be obtained by integrating the field line equations explicitly. In the case of a perturbation localized in the toroidal direction this integration can be reduced to one or a few steps. In order to investigate this situation, we start from the Hamiltonian form of the field line equations, which has been pointed out by many authors/6/,/7/, /8/. If (ψ, θ, ϕ) is the natural coordinate system of the unperturbed magnetic field $\mathbf{B}_o$ the magnetic field line equations in this coordinate system are

$$\frac{d\psi}{d\phi} = \frac{B^\psi}{B^\phi} \quad , \quad \frac{d\theta}{d\phi} = \frac{B^\theta}{B^\phi} \tag{4}$$

With the vector potential $\mathbf{A} = (0, A_\theta, A_\phi)$ the magnetic field is given by

$$\begin{aligned} B^\psi &= 1/\sqrt{g}\left(\frac{\partial A_\phi}{\partial \theta} - \frac{\partial A_\phi}{\partial \phi}\right) \\ B^\theta &= -1/\sqrt{g}\,\frac{\partial A_\theta}{\partial \psi} \\ B^\phi &= 1/\sqrt{g}\,\frac{\partial A_\theta}{\partial \psi} \end{aligned} \tag{5}$$

$g^{i,k}$ is the metric tensor of the ψ, θ, ϕ coordinate system and $\sqrt{g}\,d\psi\,d\theta\,d\phi$ the volume element. By making the following identifications $H = A_\phi$, $p = -A_\theta$ the field line equations can be written in canonical form /7/:

$$\frac{dp}{d\phi} = -\frac{\partial H}{\partial \theta} \quad , \quad \frac{d\theta}{d\phi} = \frac{\partial H}{\partial p} \tag{6}$$

p, θ are the canonical variables. The solution of these equations can be considered as a sequence of successive canonical transformations which map the point $P_k = (p_k, \theta_k)$ onto the successor $P_{k+1} = (p_{k+1}, \theta_{k+1})$ by

$$\begin{aligned} p_{k+1} &= p_k - \frac{\partial}{\partial \theta_k}\{H(\theta_k, p_{k+1}, \phi_k)\,\delta\phi\} \\ \theta_{k+1} &= \theta_k + \frac{\partial}{\partial p_{k+1}}\{H(\theta_k, p_{k+1}, \phi_k)\,\delta\phi\} \end{aligned} \tag{7}$$

$\delta\phi$ is the step size along the field line. The advantage of this procedure is that each step is area-preserving (the functional determinant of the transformation $P_k \rightarrow P_{k+1}$ is unity). This property is also maintained in the case of approximations. The question now is how to relate the generating function $H\,\delta\phi$ to the perturbation field $\mathbf{B}_1$.

In the unperturbed case the vector potential of the magnetic field is

$$\mathbf{A}_o = -\psi \nabla\theta + \int^{\psi} \iota(\psi)\, d\psi\, \nabla\phi \tag{8}$$

In the unperturbed region the Hamiltonian H_o and the momentum variable p are therefore

$$H_o = \int^{\psi} \iota(\psi)\, d\psi \quad , \quad p = \psi \tag{9}$$

Owing to the perturbation field $\mathbf{B_1}$ additional terms appear:

$$H = H_o(\psi) + A^1_\phi(\psi,\theta,\phi) \quad , \quad p = \psi + A^1_\theta(\psi,\theta,\phi) \tag{10}$$

In this case ψ and θ are no longer canonical variables, in the Hamiltonian $H(\psi,\theta,\phi)$ the variable ψ has to be replaced by p. If the toroidal component of the magnetic field B^ϕ does not vanish the second equation in (10) can always be solved for ψ and we may write

$$\psi = p - A^1_\theta(\psi(p),\theta,\phi) \tag{11}$$

The resulting Hamiltonian is

$$H(p,\theta,\phi) = H_o(p - A^1_\theta(p,\theta,\phi)) + A^1_\phi(p,\theta,\phi) \tag{12}$$

or by taking only the lowest order terms in the perturbation

$$H(p,\theta,\phi) = H_o(p) + A^1_\phi - \iota(p)\, A^1_\theta =: H_o + H_1 \tag{13}$$

Owing to our assumption of a localized perturbation the function H_1 vanishes everywhere except in a small neighbourhood of $\phi = \phi_s$. Let $\delta\phi$ be the length of this interval. In this region the main contribution to a displacement of the field line comes from the perturbation, and the transformation of the coordinates p,θ across this region is given by

$$\begin{aligned} p_2 &= p_1 - \frac{\partial}{\partial\theta_1}\{H_1(p_2,\theta_1,\phi_s)\delta\phi\} \\ \theta_2 &= \theta_1 + \frac{\partial}{\partial p_2}\{H_1(p_2,\theta_1,\phi_s)\,\delta\phi\} \end{aligned} \tag{14}$$

The index 1 indicates a point at the beginning of the perturbed region and the index 2 a point at its end. When a field line is followed once around the torus, this displacement has to be added to the unperturbed orbit described by $H_o(p)$. Outside the perturbed interval the coordinates ψ,θ are canonical variables and to describe the final map it is justified to return to these variables.

From the preceding analysis it follows that the unknown perturbation $h(\psi_1,\theta_o)$ is given by $H_1(\psi_1,\theta_o,\phi_s)\,\delta\phi$. Here the index o indicates a point in the poloidal plane $\phi = 0$ and the index 1 its image after one toroidal transit. If we write the map T in the coordinates

of the unperturbed field only the ι -profile is left to describe the different unperturbed cases. The detailed geometry,however, enters into the perturbed map $T_o + T_1$ since the function H_1 depends on the covariant components of the vector potential $\mathbf{A_1}$. The metric tensor of the coordinate system (ψ, θ, ϕ) therefore appears in H_1.

In order to obtain a rough estimate of the function h, we consider the special case with $A_\theta = 0$: the perturbation field only consists of a θ-component and a ψ-component, the ϕ- component being zero. This is no loss of generality, since the ϕ- component does not lead to displacement of the field line. The ϕ-component of $\mathbf{A_1}$ is found from

$$A_\phi = \int \sqrt{g}\, B^\psi \, d\theta$$

with $B^\psi = \vec{B}_1 \cdot \nabla\psi =: B_{1,n}|\nabla\psi|$. $B_{1,n}$ is the component of the perturbation field in the normal direction to the unperturbed magnetic surface. Neglecting the θ-dependence of g and $|\nabla\psi|$, we can approximate A_ϕ by

$$A_\phi = B_o\, \epsilon \sqrt{g} |\nabla\psi| \int f(\psi, \theta)\, d\theta$$

Here B_o is a measure of the toroidal field and ϵ is the amplitude of the perturbation field normalized to the total toroidal field B_o. The function $f(\theta)$ is of the order one and describes the poloidal variation of the perturbation field. The metric $\sqrt{g}$ and $|\nabla\psi|$ can be estimated from the volume of the magnetic surface

$$V = 2\pi a^2 R = \int \sqrt{g}\, d\psi d\theta d\phi$$

R is the major radius of the magnetic surface and a the effective minor radius. As an approximation we obtain

$$\int \sqrt{g}\, d\psi\, d\theta\, d\phi = 4\pi^2\, \psi \sqrt{g}$$

and from this relation

$$\sqrt{g}|\nabla\psi| = R\, a = A\, a^2$$

Here A is the aspect ratio of the magnetic surface. In summary the perturbation function h is

$$h(\psi, \theta) = B_o a^2\, A\, \epsilon\, f(\psi, \theta)\, \delta\phi \tag{15}$$

where f is a function of order one. The function ψ has the dimension of a magnetic flux. ψ can be made dimensionless by dividing by $B_o\, a^2$.

Then the generating function $S(\psi, \theta)$ of the map T can be written

$$S(\psi_1, \theta_o) = \psi_1 \theta_o + 2\pi \int_{\psi_1} \iota(\psi)\, d\psi + A\, \epsilon\, f(\psi_1, \theta_o)\, \delta\phi \tag{16}$$

The map described by this generating function follows from eq. (3). In order to obtain an explicit form, these equations have to be solved for ψ_1 and θ_1. If the function h is linear in ψ ($h = \psi_1\, g(\theta_o)$), the solution is trivial and we obtain the map

$$\psi_1 = \frac{\psi_o}{1 + g'(\theta_o)} \quad , \quad \theta_1 = \theta_o + 2\pi\, \iota(\psi_1) + g(\theta_o) \tag{17}$$

These equations are the basis for the numerical calculations described in the following section. As an example we consider the WVII-A stellarator with an aspect ratio of $A = 20$. Let the maximum perturbation be 30 G and the region of localisation $\delta\phi = 1/20$ which corresponds to 60 cm on the circumference. In this case the perturbation function $h(\psi, \theta)$ is of the order 10^{-3}.

IV. Results

In the WVII-A low-shear stellarator the rotational transform only varies by 1% over the plasma radius. To model this a function $\iota(\psi) = \iota_o + \iota_1\, \psi$ was chosen with $\iota_1 = 0.01$.

The perturbation $g(\theta_o)$ is written in a Fourier series:

$$g(\theta_o) = \sum_{l=1}^{15} \frac{K_l}{l} sin\, l\theta_o$$

with constants K_l given explicitly or following an exponential decay $K_l = K\, exp(-\gamma\, l)$. In this latter case the δ- like perturbation is characterised by the two parameters K and γ. These parameters are chosen such that the map yields roughly the same island pattern as found from the field line tracing taking into account the current leads to the helix /2/. The numbers are $K = 4 \times 10^{-3}$ and $\gamma = 0.2$. In fig. 4 the islands arising at $\iota = 1/2\,, \psi = 1$ are shown. The Cartesian coordinates of the plot are related to ψ, θ by $x = \sqrt{\psi}\, cos\theta\,,\ y = \sqrt{\psi}\, sin\,\theta$. Similar islands occur at $\iota = 1/3\,, 2/3\,, ...m/n$. The size of the islands increases with the perturbation parameter K and decreases with the period n, which is the number of toroidal transits before the field line closes upon itself. Since the Fourier spectrum of the perturbation contains harmonics up to $l = 15$,the first generation of islands is created at all rational surfaces with denominator $n = 1, ...15$. The size of these islands increases with the square root of the control parameter K. The first generation of islands at two rational surfaces $\iota = m_1/n_1$ and $\iota = m_2/n_2$ gives rise to a second generation of islands at $\iota = (m_1 + m_2)/(n_1 + n_2)$. Continuing this process yields a sequence of rational surfaces with $\iota_k = m_k/n_k$, where the numerator and the denominator follow a Fibonacci series. The scaling of these islands was studied in the case of two first- generation islands with K_2 and K_3, higher Fourier harmonics being set to zero. As seen from fig. 5, the first-generation island at $\iota = 1/3$ increases roughly as $\sqrt{K}$ $(K = K_2 = K_3)$. The second-generation island at $\iota = 2/5$ already shows a faster increase and the third ($\iota = 3/8$) and fourth-generation islands ($\iota = 5/13$) increase with a higher power than the preceding generation. At a fixed control parameter the size of the island decays exponentially with the period n (fig. 6). The behaviour at the chaos border, when KAM surfaces are destroyed, is determined by the high-n islands, whereas

in the subcritical case only a finite number of low-generation islands, whose width is larger than the gyroradius of electrons, affect the plasma confinement.

The general trend of islands to decrease with n may explain the dependence of confinement on ι_o in Wendelstein VII-A. The biggest islands created by external perturbations arise at $\iota = 1/2$ and $\iota = 1/3$. The neighbourhood of these rational surfaces, however, contains rational surfaces with a high period n only. Islands on these surfaces are exponentially small. In figs. 7 - 10 comparison is made with a fixed perturbation spectrum in different ι-regimes. In fig. 7 the region from $\iota = 0.45$ on the magnetic axis to $\iota = 0.47$ at the boundary is shown. The perturbation spectrum is given by $K_l = 6 \times 10^{-3}\, exp(-0.05\, l)$, $l = 1, ...15$. Islands can be seen at $\iota = 5/11, 6/13, 7/15$. In the adjacent regime $\iota = 0.47 - 0.49$, which lies closer to $\iota = 1/2$, the same perturbation does not generate visible islands (fig. 8). The figs. 9 and 10 show the ι-regime $0.44 - 0.46$ and $\iota = 0.43 - 0.45$. Similar behaviour is found slightly above $\iota = 1/2$ and in the neighbourhood of $\iota = 1/3$.

A magnification of the pictures shows smaller and smaller islands, which can be seen from figs. 10 - 13 where the regions $1.1 \leq x \leq 1.5$ and $-0.2 \leq y \leq +0.2$ are shown. The small islands arise at $\iota = m_1 + m_2/n_1 + n_2$. For example, in fig. 11 ($\iota = 0.45 - 0.46$) the two big islands occur at $\iota = 5/11$ and $\iota = 5/13$. These islands are created by the external perturbation, which contains 15 harmonics. The other smaller islands can be identified at $\iota = 11/24,\ 16/35,\ 17/37,\ 21/46$. An increase of the perturbation amplitude leads to a rapid increase of these high- generation islands and finally to stochasticity. As has been shown by MacKay /10/, all area-preserving maps locally approach a universal map with an increase of the control parameter K. This means that the general pattern of island formation and transition to stochasticity becomes independent of the details of the specific map. Consequently the general results found for the map chosen above holds for all perturbations $h(\psi, \theta)$ of the unperturbed twist map.

The effect of shear has been studied by varying the parameter ι_1 in the ι-profile. Although the size of the islands decreases with higher shear, the distance between two adjacent rational surfaces decreases faster and after approximate overlapping of the islands the region in between disintegrates into a stochastic sea. As can be seen from fig. 15, the island at $\iota = 5/11$ grows if the shear is reduced by a factor of two. This figure has to be compared with fig. 11. An increase of the shear by a factor of two reduces the distance between the islands $\iota = 5/12,\ 6/13,\ 7/15$ and the region in between becomes stochastic (fig. 16).

In the preceding analysis the perturbation is localized to an angle ψ_s in the toroidal direction. Thus the perturbation breaks the symmetry of the stellarator field which is five fold in the case of W VII-A. If the same perturbation occured in each period, its effect on island formation would be much smaller. In order to study this behaviour, the mapping process described in eq. (3) was applied to each field period. For this purpose the toroidal angle of the perturbation and its poloidal localisation have to be specified for each period. By proper choosing all parameters characterising the perturbation in each field period we can either preserve the symmetry or break the symmetry. In fig. 17 it is shown how the same perturbation which creates two islands at $\iota = 1/2$ (see fig. 4) leads to 10 small islands if it occurs in each field period. The amplitude K is 0.02, which

is five times as high as in fig. 4. If the parameters are chosen in such a way that the position of the perturbation is different in each field period, the symmetry of the system is broken and large islands appear again. This is shown in fig. 18 where the amplitude of the perturbation is the same as in fig. 4 ($K = 0.004$). A similar situation holds for every rational magnetic surface and it can be shown from the Hamiltonian form of the field line equations (eqs. 6) that a perturbation equally distributed in every field period is much less destructive than one occurring only once around the torus.

V. Conclusions

Like the problem of a kicked pendulum the effect of toroidally localised perturbations on unperturbed magnetic surfaces can be studied with a discrete map of the poloidal plane onto itself. The results show that the influence of a fixed perturbation on island formation differs according to the region of rotational transform and shear. The regions close to low-order rational surfaces $\iota = 1/2$ and $\iota = 1/3$ are less destroyed by islands than others. This might give an explanation of the good confinement observed in these regions. Two effects of islands have to be expected : one is the modification of the equilibrium and the other one the enhanced plasma diffusion. Plasma equilibrium in the presence of islands is still an unsolved problem, neither a successful analytic theory nor a numerical code having been established to deal with this problem. The presence of electric fields which follow the pattern of the islands may lead to convective cells and result in enhanced plasma losses. Also neoclassical diffusion processes should be enhanced by islands since particles can jump from island to island by Coulomb collisions. Monte Carlo simulation by R.B. White et al. /11/ have verified this effect. Although these are only qualitative considerations, they make plausible why the region with high-order rational magnetic surfaces exhibits better confinement than those with lower ones.

In estimating the effect of islands on plasma confinement the size of the islands may be a good figure of merit for the reduction of the effective plasma radius. For this purpose the size of the islands was calculated from the residues at the fixed points of the mapping. For an island at $\iota = m/n$ the fixed point was found by minimizing the distance between a point P and its image $T^n(P)$. The tangent map DT yields the Jacobian$M$ at the fixed points and from this the excentricity of the ellipses at the o-points and the angle between separatrices at the x-points can be calculated /3/. These quantities are used to estimate the radial width $\delta\psi$ of the island. The radial width of the island can only be defined approximately, since in general the separatrix consists of a stochastic region. The sum of all islands $\sum \delta\psi$ with $\delta\psi \geq 10^{-3}$ was calculated and normalized to the maximum value a of ψ. Fig. 19 shows the effective plasma cross section $\Delta = \sum \delta\psi - a$ vs ι for a fixed external perturbation with $K = 0.02$ and $\gamma = 0.2$, $\delta\iota = 0.02$. It can be seen that the effective plasma cross section defined by the area not covered by islands roughly follows the same pattern as the experimentally found confinement time or plasma energy.

There seems to be an optimum value of the shear parameter ι_1. If the shear is too small, any island can grow to an intolerable size. If the shear is too large, island overlapping leads to rapid destruction of the magnetic surfaces. In the W VII-A stellarator the shear is modified by the plasma pressure and by the pressure driven currents. In order to understand the details of the experimental results, these modifications have to be taken into account.

In principle symmetry-breaking perturbation can be avoided in stellarators. In a modular stellarator all systematic perturbations like current leads and joints can be made equal in every field period, what is left being statistical errors coming from the construction and the assembly. Internal modifications of the field due to the finite plasma pressure preserve the symmetry, and thus they should be less effective.

Acknowledgements: The author would like to thank I. Ott for preparing the MAP code and for her assistance with the numerical calculations.

REFERENCES:

/1/ H. Renner, WVII-A Team ,NI Group, Pellet Injection Group, *Proc. 10th Conf. on Plasma Physics and Contr. Nuclear Fus. Res.* London 1985, IAEA, Vienna, CN-44/D-I-1

/2/ S. Rehker, H. Wobig *Report IPP* 2/218 1974

/3/ J.M. Greene, *J. Math. Phys.* **20** (1973) 1183

/4/ J.M. Greene: in *Nonlinear Dynamics* (R.G.H. Helleman ed.) (New York Academy of Sciences, N.Y. 1980) p.80

/5/ B.V. Chirikov, *Phys. Rep.* **52**, 265 (1979)

/6/ J.R. Cary, R.G. Littlejohn: *Ann. Phys.* **151**, 1 (1983)

/7/ A. Salat: *Z. Naturforsch.* **40a**, 959-967 (1985)

/8/ M.P. Bernardin, J.A. Tataronis *J.Math.Phys* **26** (9) Sept.1985

/9/ J. Moser, *Nonlinear Problems*, ed. R.E. Langer (University of Madison Press, Madison, Wisconsin, 1963), p.139

/10/ R.S. MacKay: *Physica 7D* (1983) 283-300

/11/ R.B. White, A.H. Boozer, R. Goldston, R. Hay, J.Albert, C.F.F. Karney, *Proc. 9th Conf. on Plasma Physics and Contr. Nuclear Fus. Res.*, Baltimore 1982, IAEA, Vienna 1983, Vol. III, p.391

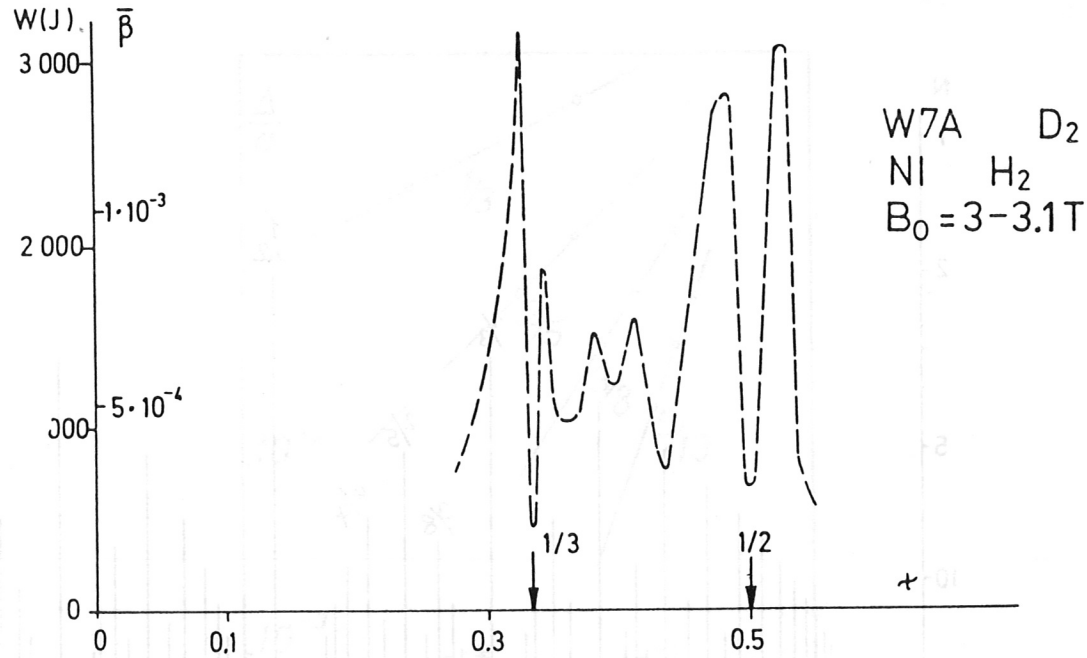

Fig. 1 : *Total plasma energy in W VII-A as a function of the external rotational transform ι_o. Heating by neutral beam injection.*

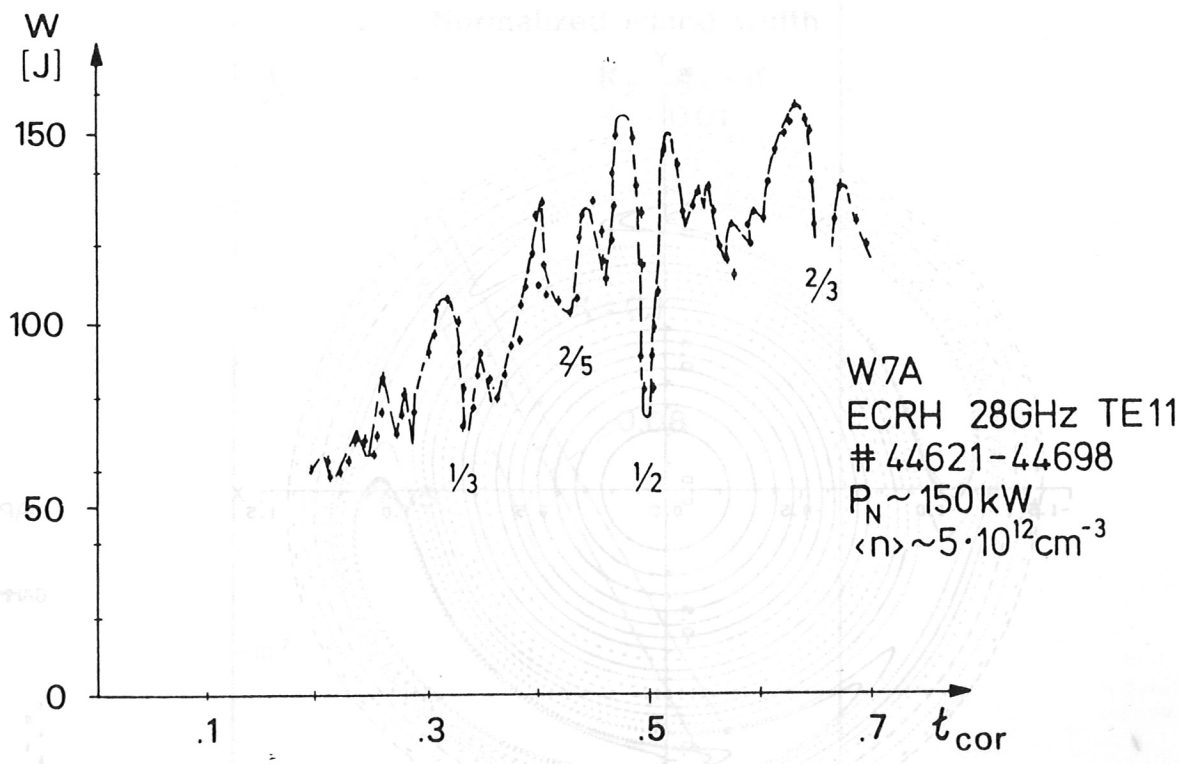

Fig. 2 : *Energy content as a function of ι_o . Electron cyclotron heating.*

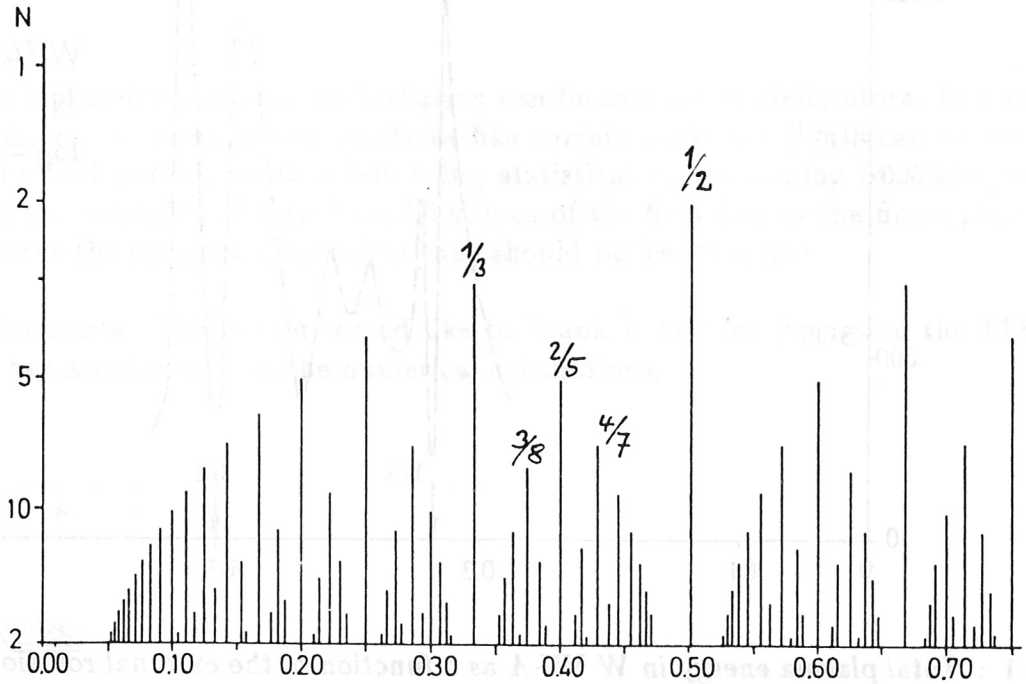

Fig. 3 : *Distribution of rational numbers. The vertical axis is* $|log\, 1/n|$, *the horizontal axis is* m/n

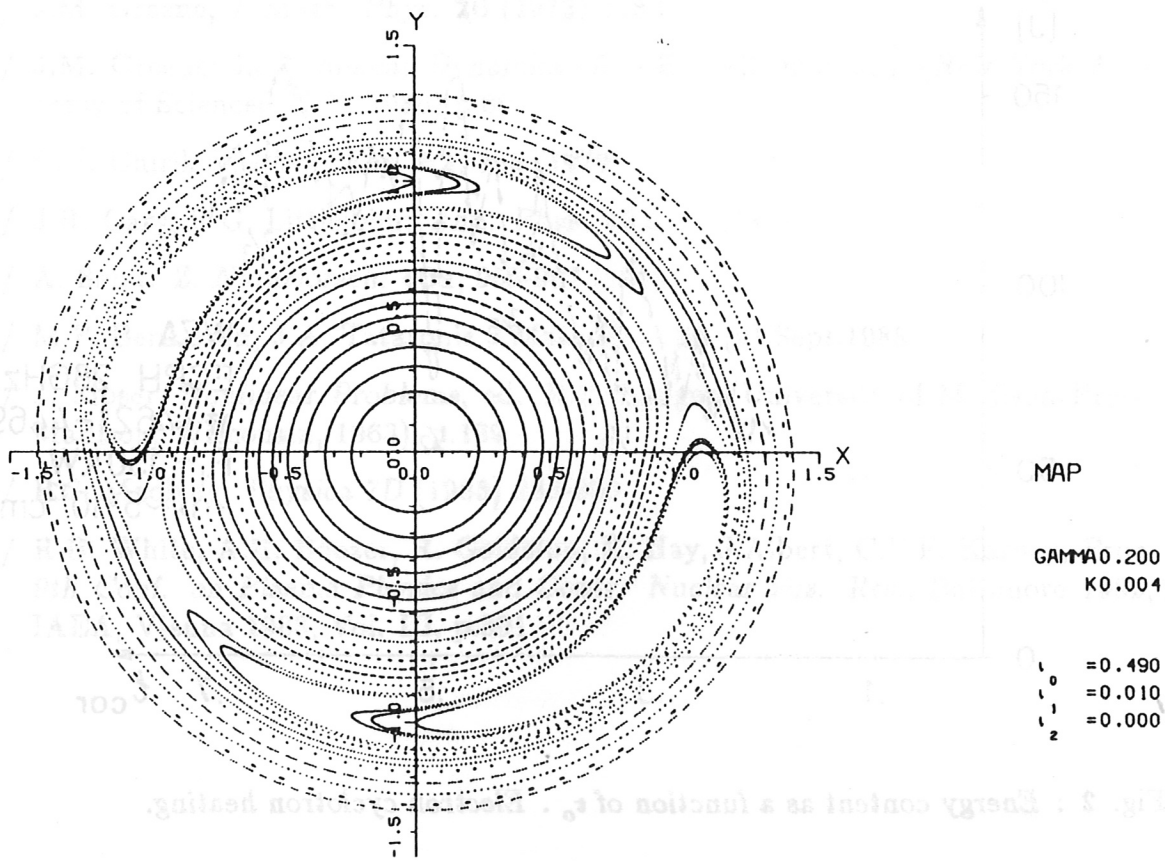

Fig. 4 : *Result of the mapping procedure following equation (17).* $t_o = 0.49, t_1 = 0.01, K = 4 \cdot 10^{-3}, \gamma = 0.2$. *The resonant surface is at* $t = 1/2$.

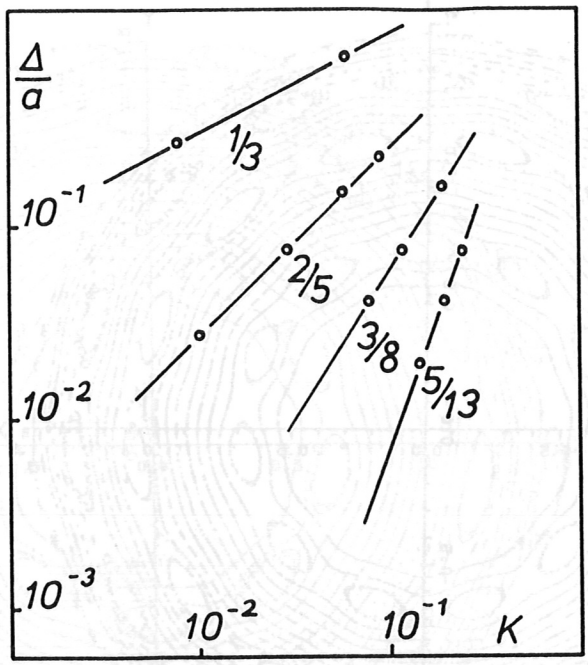

Fig. 5 : *Relative width of islands.* $t_1 = 0.01, K_2 = K_3 = K$. *The plot shows the growth of islands with the control parameter* K.

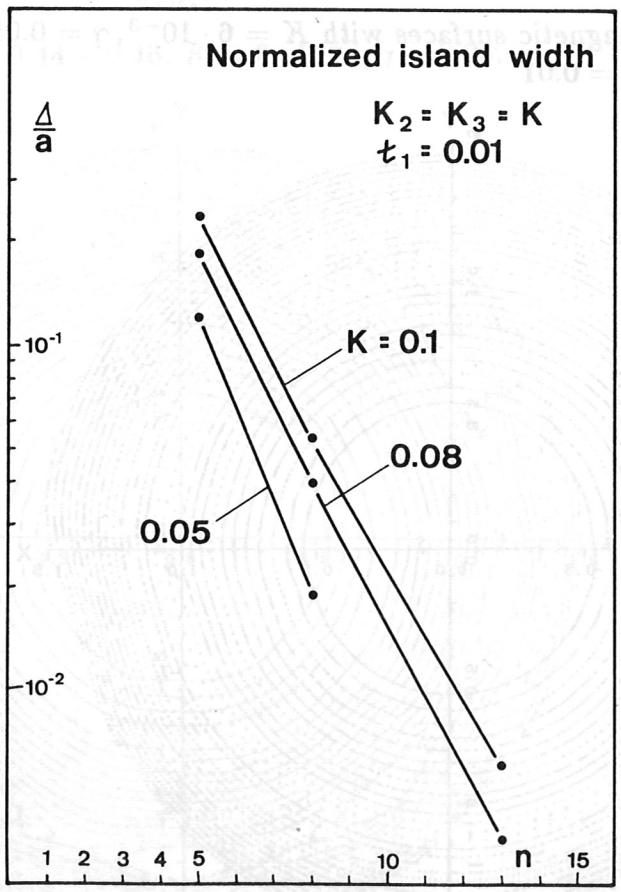

Fig. 6 : *Relative island width vs the period* n. $t_1 = 0.01, K = K_2 = K_3$

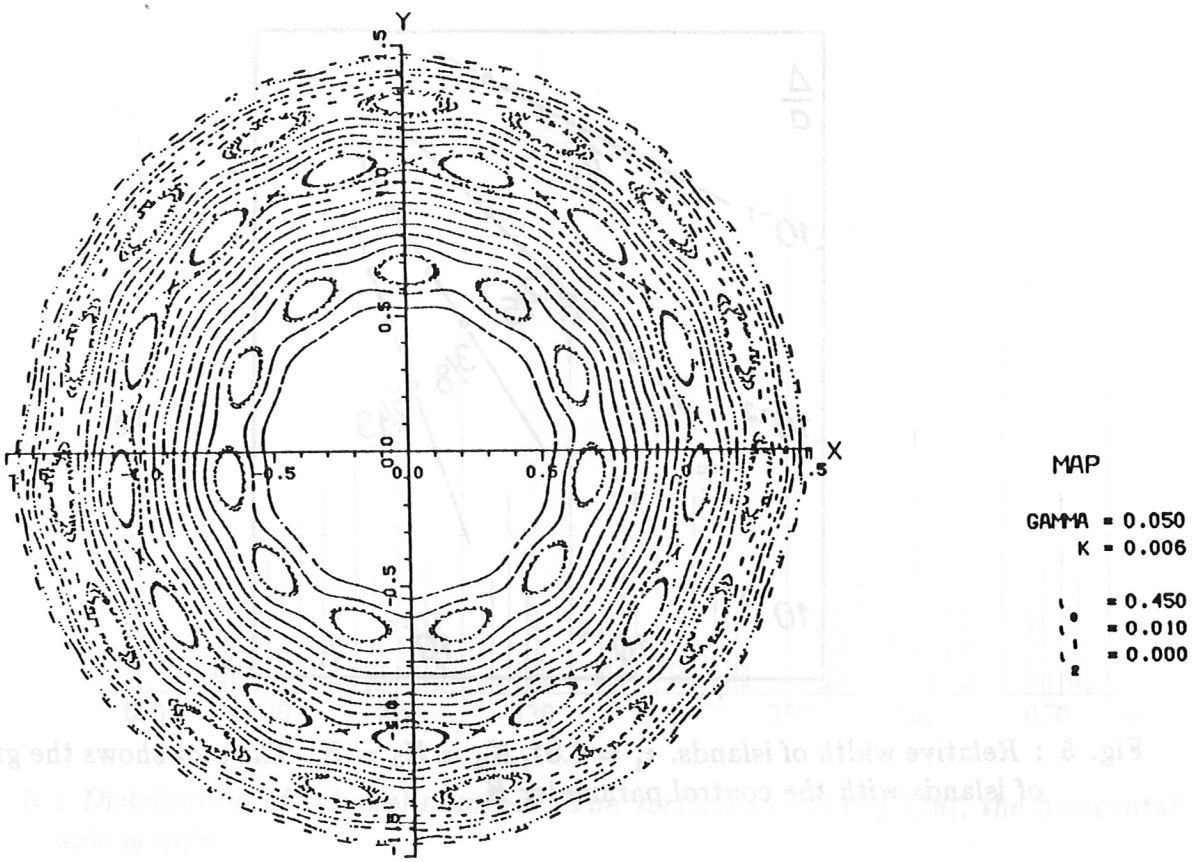

Fig. 7 : *Perturbed magnetic surfaces with* $K = 6 \cdot 10^{-3}, \gamma = 0.05$. *The regime of* ι *is* $0.45 - 0.47$. $\iota_1 = 0.01$

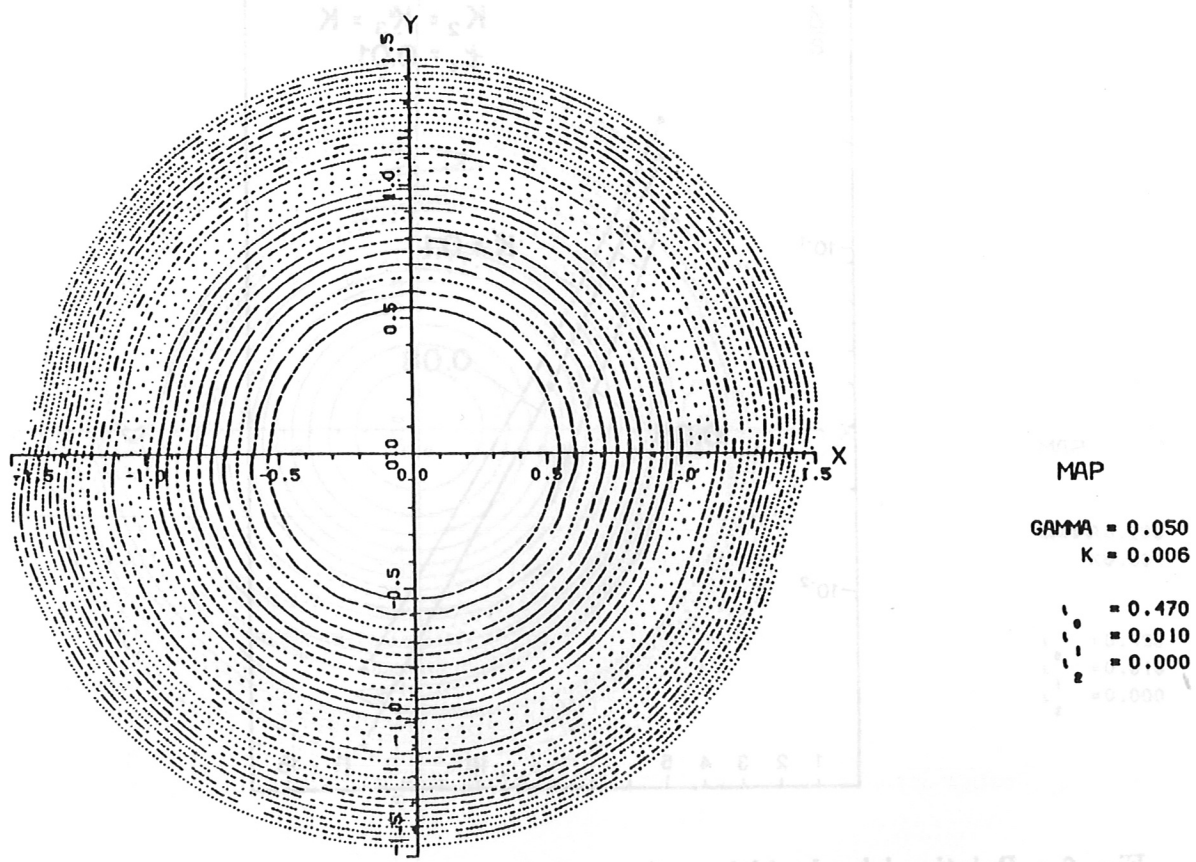

Fig. 8 : *Parameters as in fig. 7.* $\iota = 0.47 - 0.49$

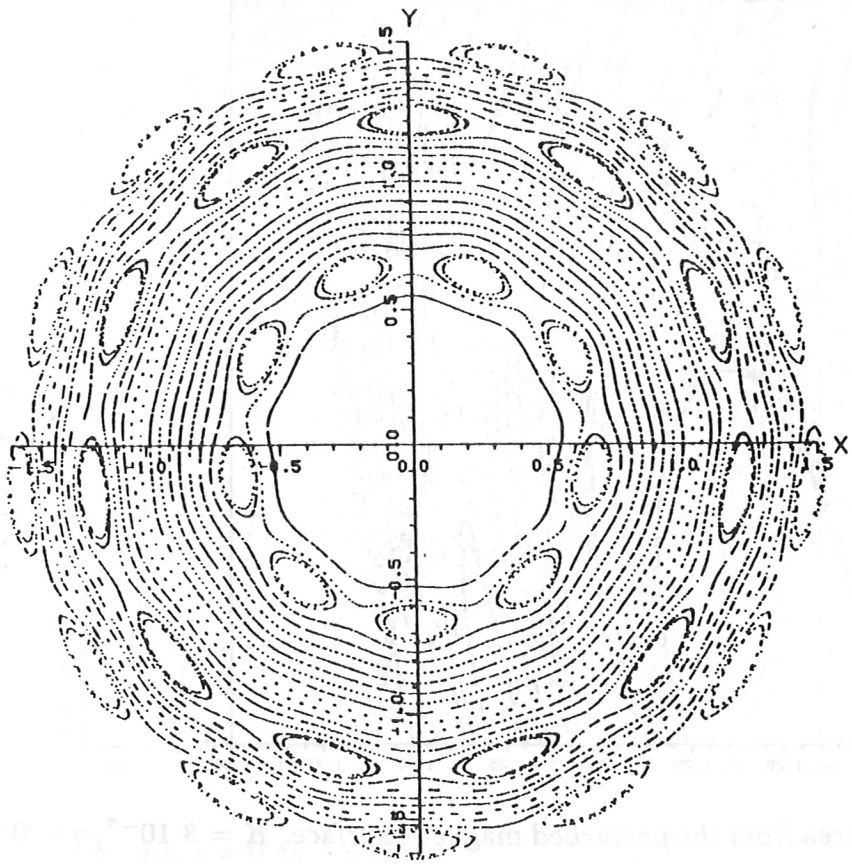

Fig. 9 : $t = 0.44 - 0.46$, $K = 6 \cdot 10^{-3}, \gamma = 0.05$.

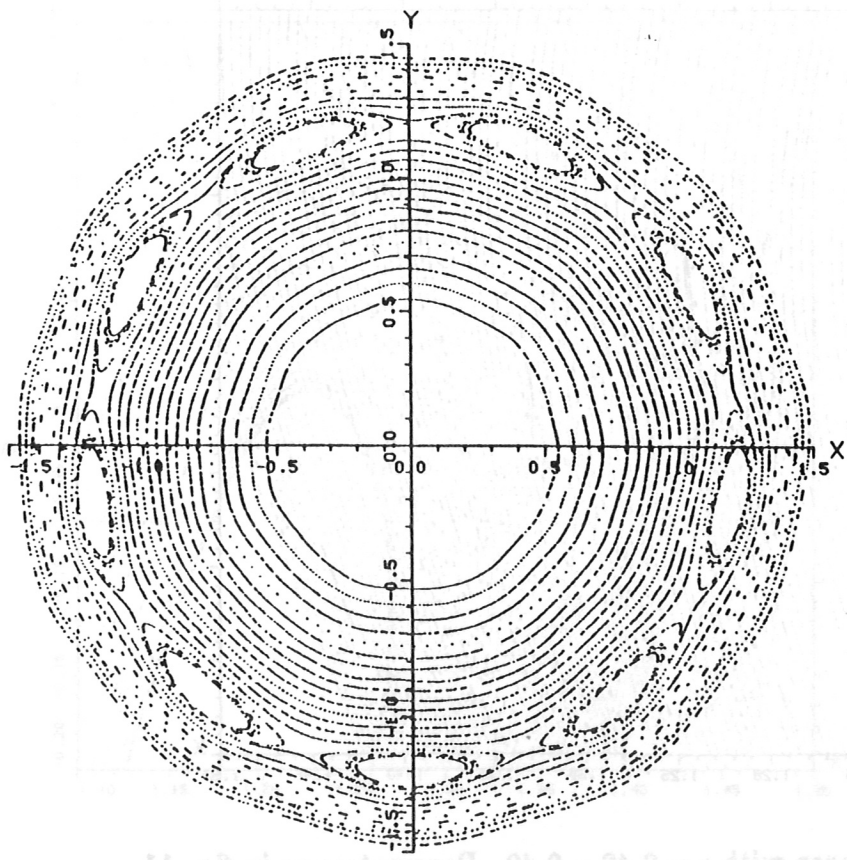

Fig. 10 : $t = 0.43 - 0.45$, $K = 6 \cdot 10^{-3}, \gamma = 0.05$

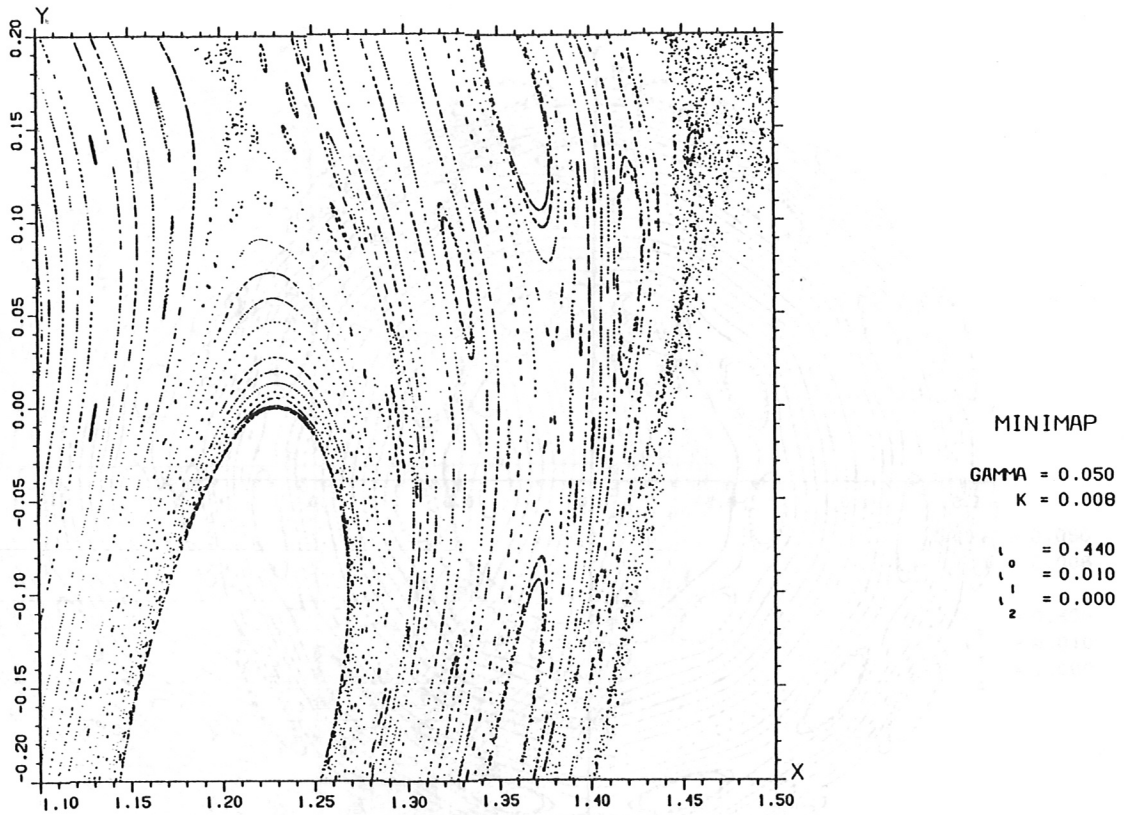

Fig. 11 : *Magnified area from the perturbed magnetic surface.* $K = 8 \cdot 10^{-3}, \gamma = 0.05, t = 0.45 - 0.46$

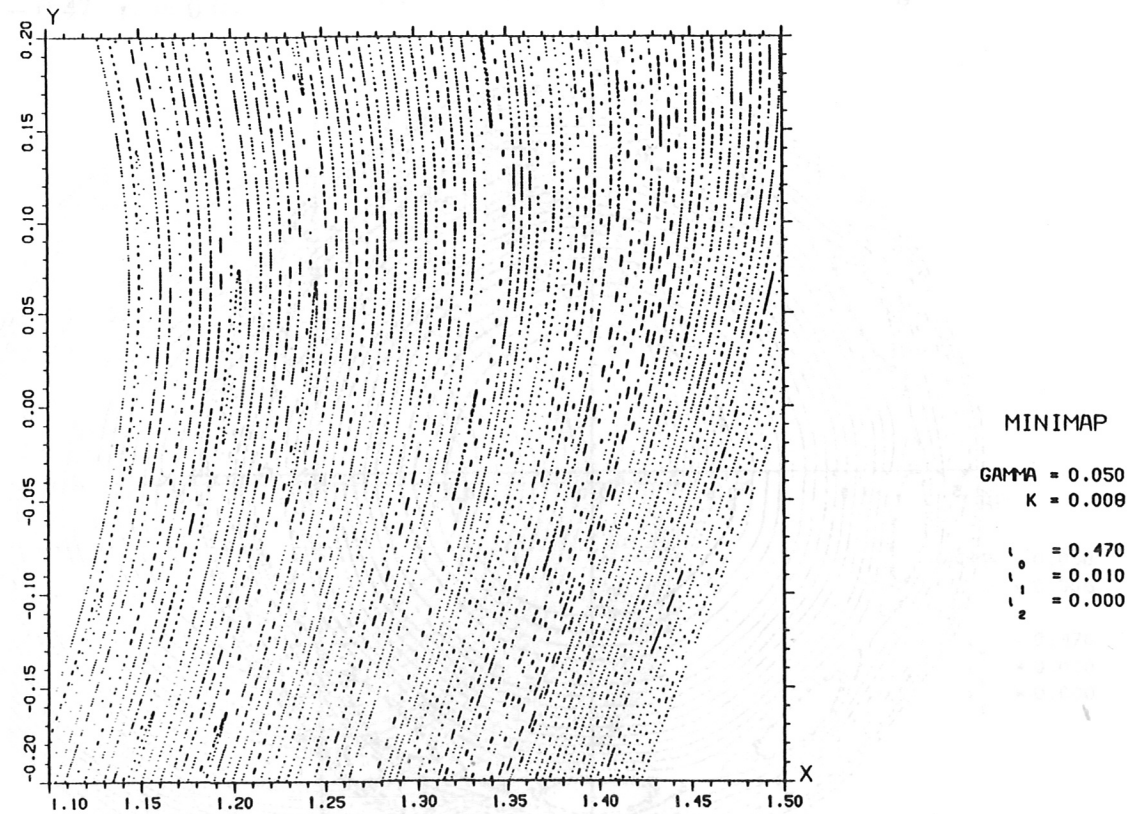

Fig. 12 : *Magnified area with* $t = 0.48 - 0.49$. *Parameters as in fig. 11.*

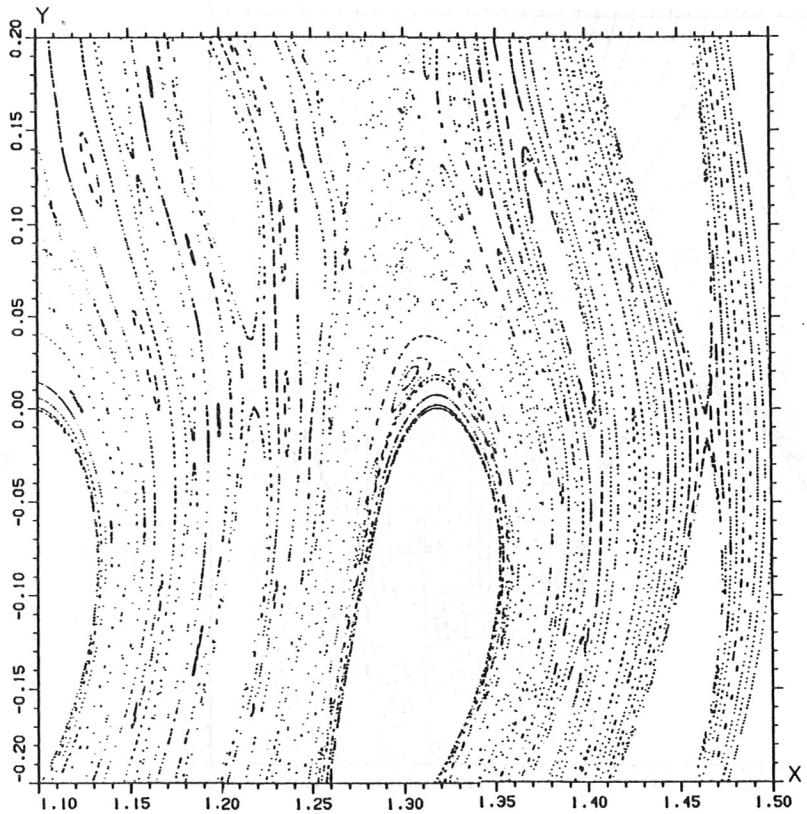

Fig. 13: $t = 0.46 - 0.47$

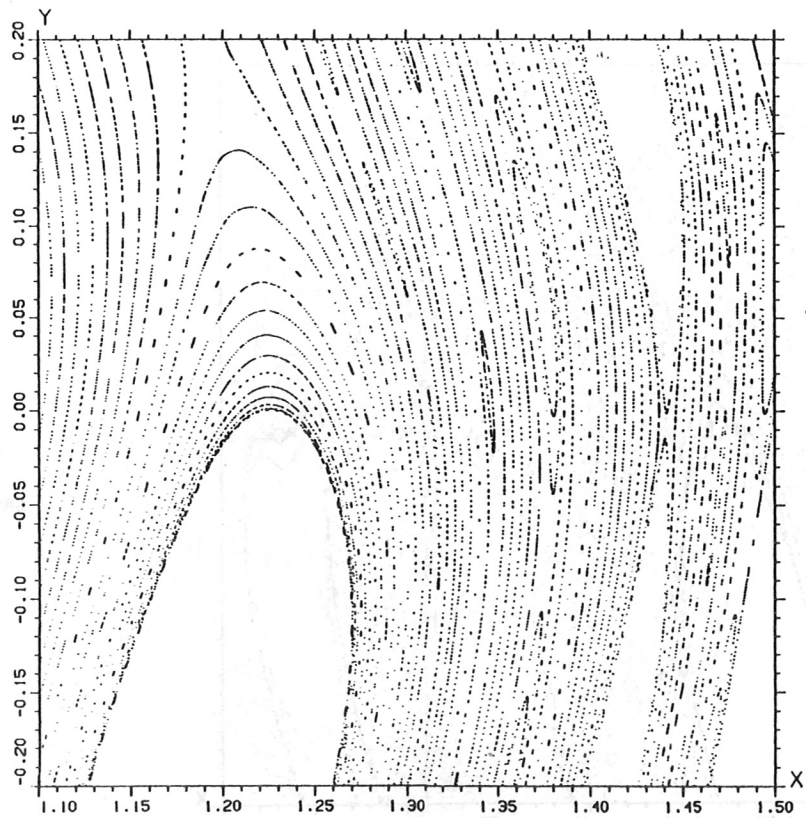

Fig. 14: $t = 0.44 - 0.45$

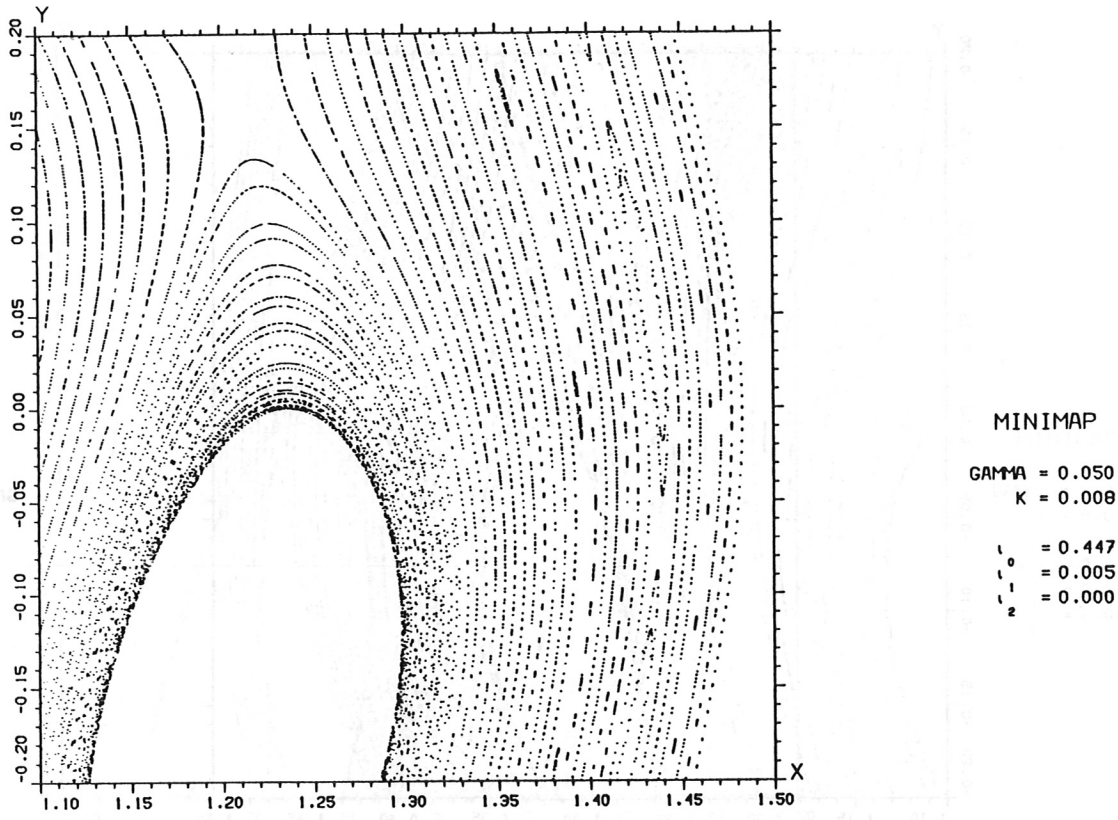

Fig. 15 : ***Reduction of shear to*** $t_1 = 0.005$. ***The big island corresponds to*** $t = 5/11$. $K = 8 \cdot 10^{-3}$, $\gamma = 0.05$

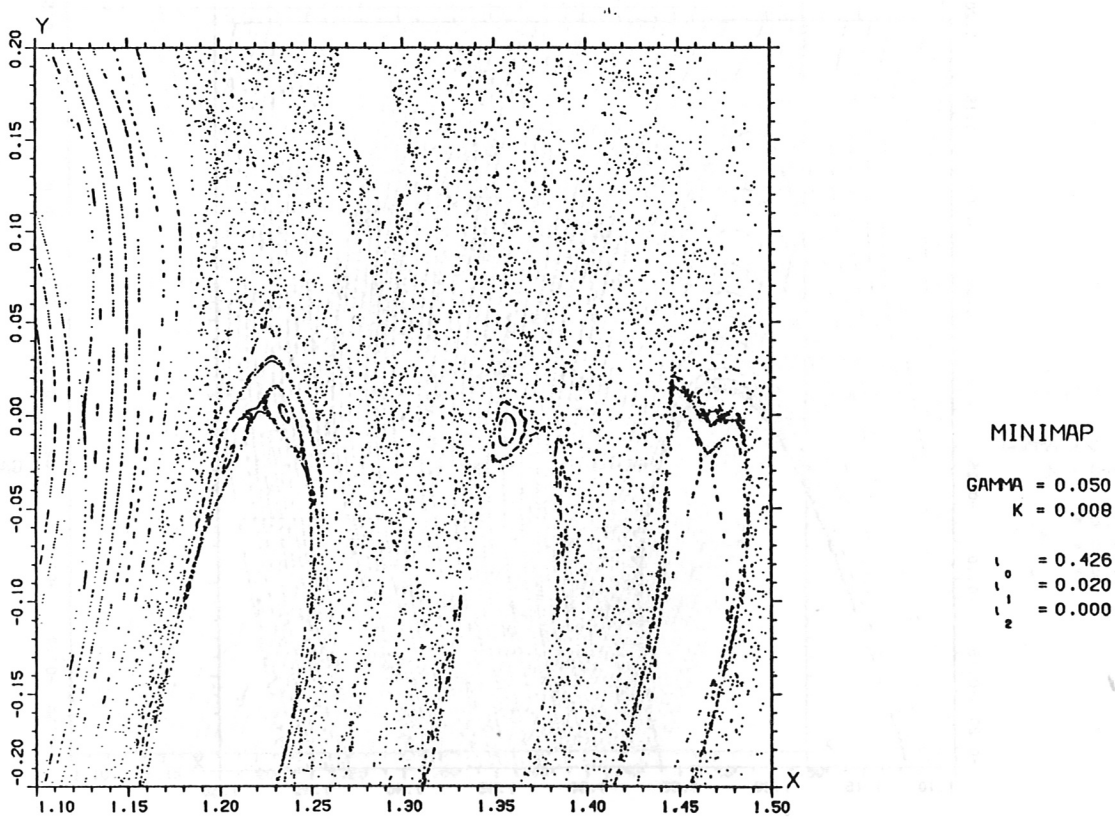

Fig. 16 : ***Effect of doubling the shear.*** $t_1 = 0.02$, $K = 8 \cdot 10^{-3}$, $\gamma = 0.05$

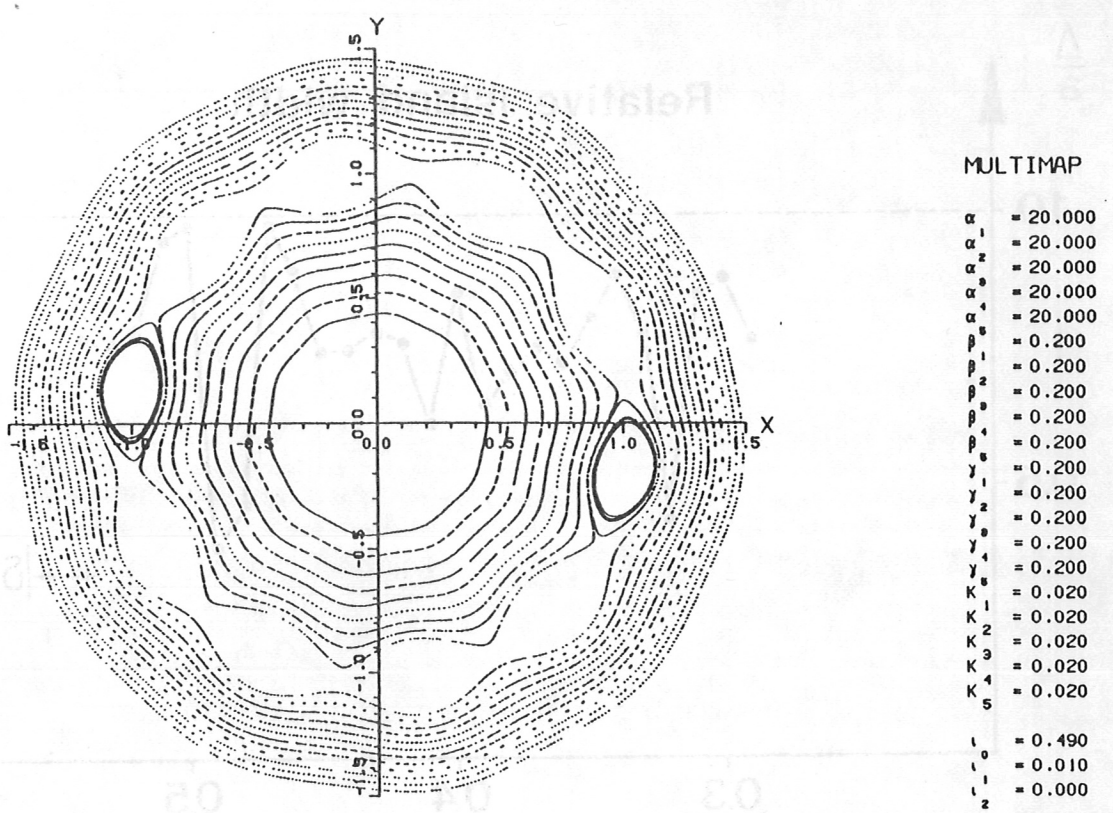

Fig. 17 : *Localized perturbation in every field period.* $\iota = 0.49 - 0.51, K = 4 \cdot 10^{-3}, \gamma = 0.2$. *The arrangement of the perturbation preserves the five-fold symmetry.*

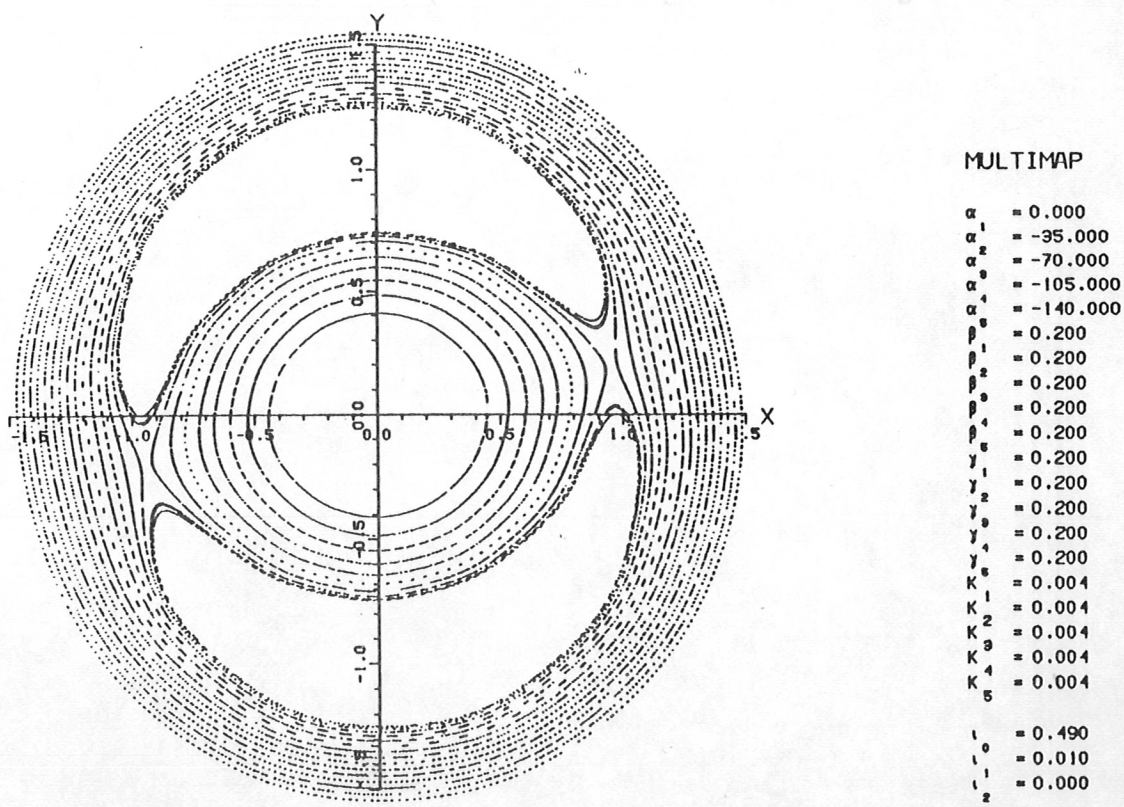

Fig. 18 : *The perturbation is identical in every field period, except for the poloidal locations. The five-fold symmetry is broken.*

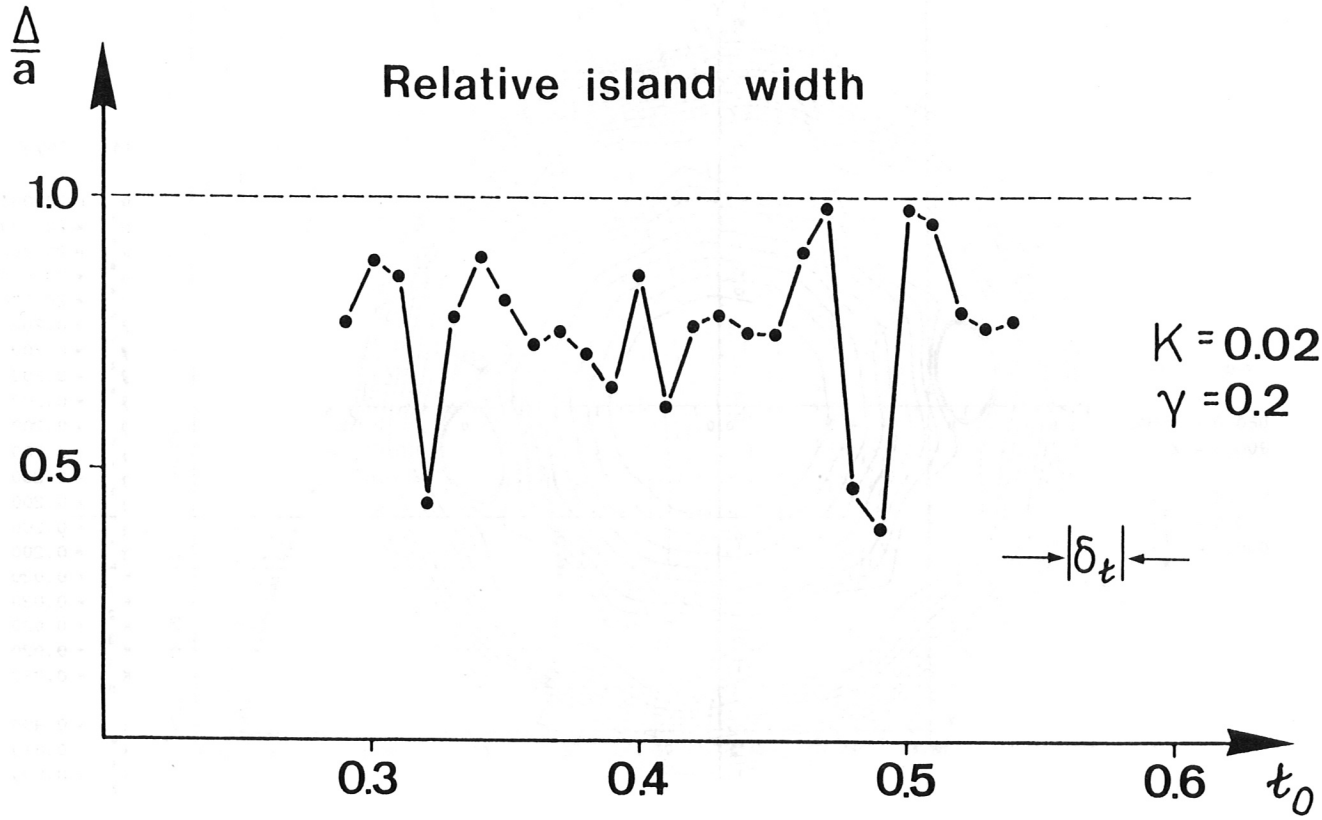

Fig. 19 : *Effective plasma radius Δ/a vs external rotational transform ι_o*